

Inverse Design of Perfectly-Matched Metamaterials

Shrey Thakkar^{#1}, Luke Szymanski^{#2}, Jorge Ruiz-Garcia^{#3}, Gurkan Gok^{*4}, Anthony Grbic^{#5}

[#]Department of Electrical Engineering and Computer Science, University of Michigan, Ann Arbor, USA

^{*}Raytheon Technologies Research Center, East Hartford, USA

{¹shreyt, ²lszym, ³jruizgar, ⁵agrbc}@umich.edu, ⁴gurkan.gok@rtx.com

Abstract—In this work, inverse design is used to develop inhomogeneous, anisotropic 2D metamaterials (electrical networks) that perform specified electromagnetic field transformations. The unique feature of the proposed metamaterials is that all their unit cells are impedance matched to each other, as well as to the surrounding space. These perfectly-matched metamaterials, unlike absorptive perfectly matched layers (PMLs), are lossless and passive. As an example, a 2D metamaterial that collimates the field of a point source excitation is reported.

Keywords—metamaterials, inverse design, transformation optics, perfectly matched layer

I. INTRODUCTION

There has been growing interest in employing inverse design strategies to devise electromagnetic (EM) metamaterials, metasurfaces and metastructures that perform complex functions [1]. Numerous devices including antenna beamformers [2], microwave circuit components [3, 4] and analog signal processors [2, 5] have been developed using inverse design methods. Inverse design is a powerful tool that can navigate high-dimensional design spaces typical to these devices, and identify solutions to nonconvex problems. The identified solutions are often not unique, allowing for the inclusion of multiple constraints and objectives. Constraints dictate the manner in which an inverse-designed electromagnetic structure achieves a desired function. For example, if a device allows reflections between its constitutive elements, it may exploit standing waves within its structure to achieve a desired function. This, in turn, can limit bandwidth and contribute to added losses [2]. These limitations can be addressed, to a certain extent, through a judicious choice of a multi-objective cost function. However, multiple objectives can also increase computational complexity or the electrical size of the structure.

This work focuses on the inverse design of inhomogeneous, anisotropic metamaterials consisting of perfectly-matched unit cells (see Fig. 1). That is, all unit cells comprising the metamaterial are impedance matched to each other under all possible excitations. In addition, the unit cells are impedance matched to the external medium surrounding the metamaterial. As a result, the metamaterial's performance does not rely on inter-cell reflections, but rather refractive effects to perform a prescribed electromagnetic function.

Lossless, reciprocal, and passive materials that are perfectly matched [6] are characteristic to transformation optics (TO) designed devices [7, 8]. In transformation optics, a desired field distribution is derived from an initial field distribution through a coordinate transformation, which directly translates to

changes in the permittivity and permeability of the underlying medium. This transformed medium is often inhomogeneous and anisotropic, but exhibits the unique property of remaining reflectionless (impedance matched) to the surrounding medium. This property is key to TO devices such as invisibility cloaks [9]. The perfectly matched property of TO devices was analyzed in [6] and a general form for the material parameters that enable perfect matching was derived.

In practice, discretizing the transformed medium to realize TO devices deteriorates their impedance-matched property. An alternative design approach was proposed in [10], where discrete blocks (unit cells) of homogeneous, anisotropic material within a 2-D lattice are designed to locally control phase progression and power flow direction [11]. Combining this approach with perfectly-matched unit cells [6] allows for intuitive and reflectionless device design, and lays the foundation for this work.

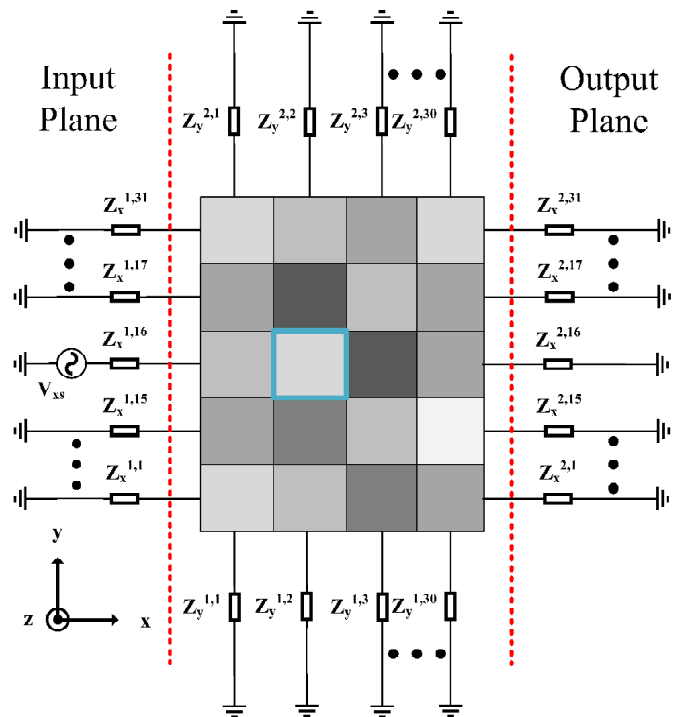


Fig. 1. Proposed spatially variant metamaterial, discretized into a 31 (rows) \times 30 (columns) grid consisting of discrete blocks of homogeneous, anisotropic media.

In this paper, an equivalent circuit for unit cells of a perfectly-matched material [12] is derived. Then, a circuit-based optimizer employing the adjoint variable method [2] is

used to design reflectionless, 2D metamaterials (circuit networks) that perform a desired electromagnetic field transformation, as shown in Fig. 1. The proposed inverse-designed metamaterials are devoid of internal (inter-cell) reflections and perfectly impedance matched to the surrounding medium. As a result, these refractive devices depend only on path length, and therefore promise true time-delay performances and broadband operation. Since the devices are inverse designed, practical constraints can be integrated into their design. In addition, multiple-input multiple-output functionality or multiple field transformations may be possible, unlike in TO.

This paper is arranged as follows: First, the general form of the material parameters (see Fig. 2(a)) needed for perfect matching is reviewed. Next, a 2D transmission-line unit cell (see Fig. 2(b)) is introduced that models perfectly-matched media. Finally, the inverse design of a perfectly-matched metamaterial is reported. The device transforms a point source excitation to a collimated beam with a trapezoidal amplitude taper. Concluding remarks follow.

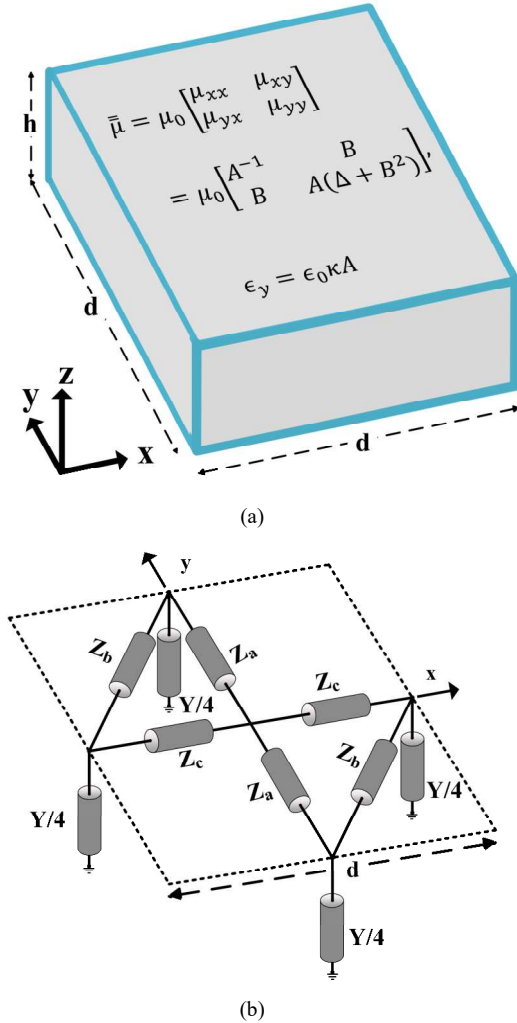


Fig. 2. Unit cell models: (a) Block of homogeneous, anisotropic media within the metamaterial (see Fig. 1); (b) Equivalent TL circuit in Bowtie Topology.

II. PERFECTLY MATCHED MATERIAL PARAMETERS

In this section, we review the general form of the material parameters for a lossless and passive anisotropic medium (shown in Fig. 2(a)) that exhibits perfect matching. Consider a TE-polarized plane wave incident on a planar interface, in the y - z plane, separating two semi-infinite, homogeneous, lossless, magnetically anisotropic media. Consistent with the assumed polarization, the electric field is z -directed, and the magnetic field lies in the x - y plane. No variation is assumed along z . It can be shown that the following conditions ensure that the normal TE wave impedances of both media remain impedance matched for all angles of incidence [6]

$$|\bar{\mu}|_1 = |\bar{\mu}|_2 = \Delta, \quad (\mu_{xx}\epsilon_z)_1 = (\mu_{xx}\epsilon_z)_2 = \kappa. \quad (1)$$

where $|\bar{\mu}|_1$ and $|\bar{\mu}|_2$ are the determinants of the permeability tensors in medium 1 and 2, respectively, ϵ_z is the scalar permittivity, and $(\mu_{xx}\epsilon_z)_1$ and $(\mu_{xx}\epsilon_z)_2$ represent the normal refractive indices in each medium. Consequently, the general form of the material parameters that follow from (1) are

$$\begin{bmatrix} \mu_{xx} & \mu_{xy} \\ \mu_{yx} & \mu_{yy} \end{bmatrix} = \begin{bmatrix} A^{-1} & B \\ B & A(\Delta + B^2) \end{bmatrix}, \quad (\epsilon_z) = \kappa A \quad (2)$$

where A and B are real numbers. In this work, the metamaterials considered will be impedance matched to free space. Therefore,

$$\Delta = 1, \quad \kappa = 1. \quad (3)$$

In summary, media with material parameters of the form described by (2) and (3) are impedance matched to each other as well as to free space for all TE excitations.

III. EQUIVALENT TENSOR TL CIRCUIT FOR A PERFECTLY MATCHED MATERIAL

In this section, an equivalent circuit (tensor transmission-line) model for a square block of a perfectly-matched material, given by (2), is presented.

A. Tensor Transmission-Line Unit Cell

A tensor transmission-line metamaterial unit cell of a shunt node configuration is shown in Fig. 2(b). It represents an anisotropic medium under a TE excitation [12]. The impedances Z_c and Z_a represent the series impedances along the x and y axes, while Z_b represents the series impedance along the x - y diagonal. The shunt admittance Y represents the shunt branch of the unit cell.

The propagation characteristics of a periodic network consisting of unit cells depicted in Fig. 1 can be completely characterized in terms of a series impedance tensor and scalar admittance,

$$\bar{\bar{Z}} = \begin{bmatrix} Z_{xx} & Z_{xy} \\ Z_{yx} & Z_{yy} \end{bmatrix}, \quad Y \quad (4)$$

when the phase delay across the unit cell is small. In this limit, the impedance tensor $\bar{\bar{Z}}$ becomes,

$$\bar{\bar{Z}} = \begin{bmatrix} \frac{2Z_c(Z_a+Z_b)}{Z_a+Z_b+Z_c} & -\frac{2Z_aZ_c}{Z_a+Z_b+Z_c} \\ -\frac{2Z_aZ_c}{Z_a+Z_b+Z_c} & \frac{2Z_c(Z_a+Z_b)}{Z_a+Z_b+Z_c} \end{bmatrix}. \quad (5)$$

Next, a one-to-one relationship is established between a material, with parameters given by (2) (see Fig. 2(a)), and the circuit network, shown in Fig. 2(b), with circuit parameters given by (4) and (5), for TE-polarization.

B. Circuit – Material Equivalence

Propagation along the periodic electrical network shown in Fig. 1 can be directly related to TE-wave propagation within an anisotropic medium with a full 2×2 permeability tensor and scalar permittivity in the following manner [6],

$$j\omega d \begin{bmatrix} \mu_{yy} & -\mu_{xy} \\ -\mu_{yx} & \mu_{xx} \end{bmatrix} = \begin{bmatrix} Z_{xx} & Z_{xy} \\ Z_{yx} & Z_{yy} \end{bmatrix}, \quad j\omega d \epsilon_z = Y, \quad (6)$$

where d represents the dimension of a unit cell in the periodic electrical network (see Fig. 2). Using (2) and (5), a perfectly-matched circuit network's series impedances can be expressed in terms of the material parameter variables A , B and Δ as

$$\begin{aligned} Z_a &= \frac{j\omega d \Delta}{2[A(\Delta + B^2) - B]}, \\ Z_b &= \frac{j\omega d \Delta}{2B}, \\ Z_c &= \frac{j\omega d A \Delta}{2(1 - AB)} \end{aligned} \quad (7)$$

and the shunt admittance can be represented as,

$$Y = j\omega d \kappa A. \quad (8)$$

The series and shunt circuit impedances are imaginary for real values of A and B . However, for imaginary A and B values, the shunt and series impedances become real valued (lossy). This results in a perfectly-matched lossy network, as in the case of a Perfectly Matched Layer (PML) used in computational electromagnetics [13].

IV. DESIGN EXAMPLE: A COLLIMATOR WITH AMPLITUDE CONTROL

In this section, inverse design is used to devise a metamaterial (2D electrical network) composed of perfectly-matched tensor transmission-line unit cells, shown in Fig. 2(b). The unit cells of the 2D, spatially variant electrical network are of the form given by (7) and (8). The metamaterial transforms a point source excitation to a collimated wavefront with a trapezoidal amplitude taper. It allows for precise and independent control of the amplitude and phase of the output field. This is in contrast to typical gradient index lenses that do not provide amplitude control of the collimated beam and are not impedance matched.

The metamaterial, depicted in Fig. 1, is assumed to be lossless and consists of a 31×30 grid of transmission-line unit cells of the form shown in Fig. 2(b). Each unit cell represents a block of a perfectly-matched medium shown in Fig. 2(a). The metamaterial is designed to operate at 10 GHz and is comprised

of unit cells that are $\lambda_0/15$ in dimension. Therefore, the width of the metamaterial is $2.067\lambda_0$ and its depth is $2\lambda_0$. The input and output planes of the metamaterial are separated by the depth. A single node at the center of the input plane is excited by a 34.3 V voltage source with source resistance equal to 147Ω . This is chosen such that the maximum power available from the source is 1 W. The remaining unit cells along the perimeter of the metamaterial are terminated with free space wave impedance, 377Ω , in accordance with the constraint imposed by (3). From (3), (7), and (8), it is apparent that each unit cell has 2 degrees of freedom: A and B . These degrees of freedom provide independent control over phase progression and power flow within each unit cell. The upper and lower bounds for both variables are chosen such that they can be practically realized as following: $A: -1 \rightarrow 5$, $B: -2 \rightarrow 2$. Since the output voltage profile is chosen to be symmetric, we impose symmetry across the centre row ($x = 16$ in Fig. 1). This reduces the number of design variables in the grid to 960 variables.

To inverse design the metamaterial, we utilize the circuit optimizer reported in [2] with the excitation, desired output (aperture) voltage profile (Fig. 4(c)), the unit cell model, shown in Fig. 2(b), with circuit parameters given by (3), (7) and (8), and the stated perimeter terminations. The optimizer also requires initial values for the design variables which are set to: $A = 1$, $B = 0$. Therefore, the initial values are representative of free space. The optimizer is then used to minimize a cost function that penalizes a mismatch between the target and the device's output voltage profile. The optimized spatial distributions for A and B are shown in Fig. 3.

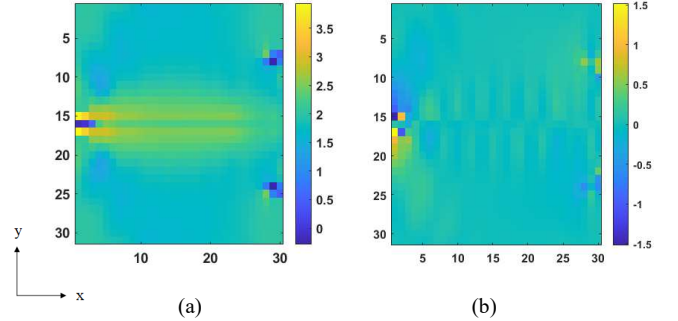


Fig 3. 2D plots of the optimized parameters over the metamaterial. (a) Parameter A ; (b) Parameter B .

From Fig. 3, it is observed that the material parameters are largely adiabatic, with localized regions of extreme inhomogeneity near the source on the input plane and along the output plane (see Fig. 1). Near the source, the extreme inhomogeneity prevents loss of power to the terminations along the input plane. In the output region, the extreme inhomogeneity manipulates the field to achieve the desired voltage profile at the output plane.

From Fig. 2(b), we note that each unit cell has two terminals aligned with the x -axis and two aligned with the y -axis. The voltage magnitude and phase at terminals aligned with the x -axis are plotted in Fig. 4(a) and 4(b), respectively. The plots show that the network initially focuses the field into the center of the metamaterial (between unit cells 8 and 25 along the x -axis). Then, it manipulates the field to achieve the desired

trapezoidal amplitude taper at the output plane. Additionally, the phase of the field is collimated as in the case of a gradient index lens. The amplitude and phase profiles of the voltage along the output plane achieved by the metamaterial are in excellent agreement with the target output profile, as seen in Fig. 4(c). The power delivered to the metamaterial by the source is 1 W, and the input impedance seen by the source is 148.32 Ω . The power exiting the output plane is 69% of the power delivered by the source. Therefore, 31% of the power was lost to terminations along the perimeter of the metamaterial (upper, lower, and input boundaries in Fig. 4(a)). This power loss can be further limited by altering the cost function.

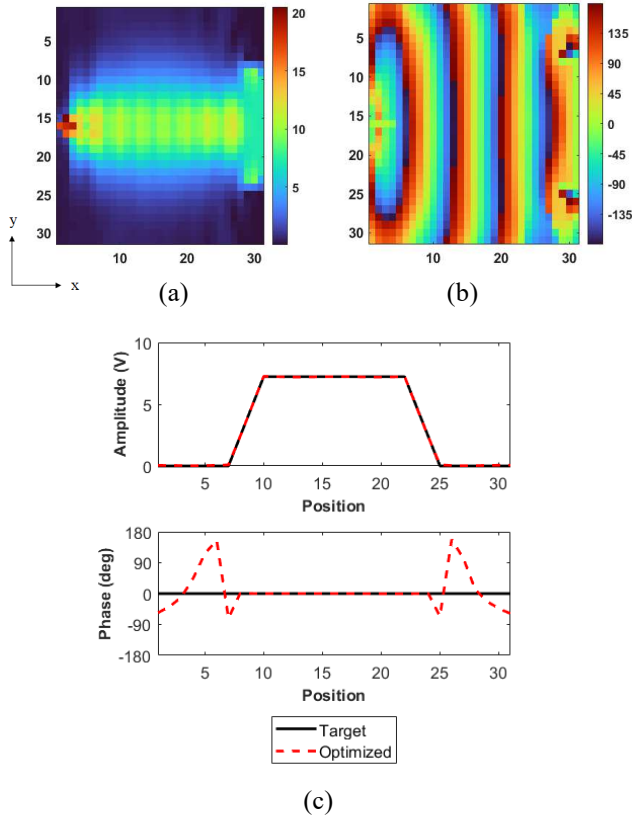


Fig. 4. Simulated voltages at nodes within the metamaterial. (a) Simulated voltage magnitude and (b) Simulated voltage phase at terminals aligned with the x-axis. (c) Desired (solid black line) and achieved (red dashed line) voltage profile at the output plane. Note: The voltage phase values at points where the voltage magnitude is zero are irrelevant.

V. CONCLUSION

In this paper, perfectly-matched, lossless, and passive media were reviewed and a tensor transmission-line (circuit network) representation for such media was derived. Inverse design was then applied to design a perfectly-matched metamaterial (2D electrical network). The proposed perfectly-matched metamaterials and their inverse design provide a new paradigm for the design of electromagnetic devices with complex functionalities. To demonstrate the effectiveness of the method, the design of a metamaterial is reported that transforms a point source excitation to a collimated wavefront with trapezoidal amplitude taper in a reflectionless manner.

ACKNOWLEDGMENT

L. Szymanski is currently with the MIT Lincoln Laboratory, Lexington, USA. This work was supported by the National Science Foundation through the Grant Opportunities for Academic Liaison with Industry (GOALI) Program under Grant 1807940.

REFERENCES

- [1] Z. Li, R. Pestourie, Z. Lin, S. G. Johnson, and F. Capasso, "Empowering Metasurfaces with Inverse Design: Principles and Applications," *ACS Photonics*, vol. 9, no. 7, pp. 2178–2192, Jul. 2022, doi: 10.1021/acsphotonics.1c01850.
- [2] L. Szymanski, G. Gok, and A. Grbic, "Inverse Design of Multi-Input Multi-Output 2-D Metastructured Devices," *IEEE Trans. Antennas Propag.*, vol. 70, no. 5, pp. 3495–3505, May 2022, doi: 10.1109/TAP.2021.3137301.
- [3] M. Sedaghat, R. Trinchero, and F. Canavero, "Compressed Machine Learning-Based Inverse Model for the Design of Microwave Filters," in *2021 IEEE MTT-S International Microwave Symposium (IMS)*, Atlanta, GA, USA, Jun. 2021, pp. 13–15, doi: 10.1109/IMS19712.2021.9574884.
- [4] Z. Liu, E. A. Karahan, and K. Sengupta, "Deep Learning-Enabled Inverse Design of 30–94 GHz P_{sat,3dB} SiGe PA Supporting Concurrent Multiband Operation at Multi-Gb/s," *IEEE Microw. Wireless Compon. Lett.*, vol. 32, no. 6, pp. 724–727, Jun. 2022, doi: 10.1109/LMWC.2022.3161979.
- [5] A. S. Backer, "Computational inverse design for cascaded systems of metasurface optics," *Opt. Express*, vol. 27, no. 21, p. 30308, Oct. 2019, doi: 10.1364/OE.27.030308.
- [6] G. Gok and A. Grbic, "A physical explanation for the all-angle reflectionless property of transformation optics designs," *J. Opt.*, vol. 18, no. 4, p. 044020, Apr. 2016, doi: 10.1088/2040-8978/18/4/044020.
- [7] J. B. Pendry, D. Schurig, and D. R. Smith, "Controlling Electromagnetic Fields," *Science*, vol. 312, no. 5781, pp. 1780–1782, Jun. 2006, doi: 10.1126/science.1125907.
- [8] D.-H. Kwon and D. H. Werner, "Transformation Electromagnetics: An Overview of the Theory and Applications," *IEEE Antennas Propag. Mag.*, vol. 52, no. 1, pp. 24–46, Feb. 2010, doi: 10.1109/MAP.2010.5466396.
- [9] W. Yan, M. Yan, Z. Ruan, and M. Qiu, "Coordinate transformations make perfect invisibility cloaks with arbitrary shape," *New J. Phys.*, vol. 10, no. 4, p. 043040, Apr. 2008, doi: 10.1088/1367-2630/10/4/043040.
- [10] G. Gok and A. Grbic, "Tailoring the Phase and Power Flow of Electromagnetic Fields," *Phys. Rev. Lett.*, vol. 111, no. 23, p. 233904, Dec. 2013, doi: 10.1103/PhysRevLett.111.233904.
- [11] G. Gok and A. Grbic, "Alternative Material Parameters for Transformation Electromagnetics Designs," *IEEE Trans. Microw. Theory Techn.*, vol. 61, no. 4, pp. 1414–1424, Apr. 2013, doi: 10.1109/TMTT.2013.2248018.
- [12] G. Gok and A. Grbic, "Tensor Transmission-Line Metamaterials," *IEEE Trans. Antennas Propag.*, vol. 58, no. 5, pp. 1559–1566, May 2010, doi: 10.1109/TAP.2010.2044351.
- [13] J.-P. Berenger, "A perfectly matched layer for the absorption of electromagnetic waves," *Journal of Computational Physics*, vol. 114, no. 2, pp. 185–200, Oct. 1994, doi: 10.1006/jcph.1994.1159.